

Infrared Properties of  $\text{CaF}_2$ ,  $\text{SrF}_2$ , and  $\text{BaF}_2$ W. KAISER, W. G. SPITZER, R. H. KAISER, AND L. E. HOWARTH  
*Bell Telephone Laboratories, Murray Hill, New Jersey*

(Received May 10, 1962)

Reflectivity and transmission measurements on  $\text{CaF}_2$ ,  $\text{SrF}_2$ , and  $\text{BaF}_2$  have been studied to obtain information on the lattice vibrations. The reflection band in each material has been analyzed with classical dispersion theory. In order to fit the data, it was necessary to use one strong and one weak resonance in each case. The strong resonance is identified as the transverse optical mode of vibration for zero wave vector and is at 38.9, 46.1, and 54.3  $\mu$  for  $\text{CaF}_2$ ,  $\text{SrF}_2$ , and  $\text{BaF}_2$ , respectively. The long-wavelength value for the dielectric constant obtained from the optical measurements indicated a disagreement with the published value for  $\text{SrF}_2$  obtained from capacity measurements. Capacity measurements were made and showed the previously accepted value for  $\text{SrF}_2$  to be in error. The transverse optical-mode frequencies are shown to agree very well with the spacing of some of the satellite lines in the emission spectrum of  $\text{Sm}^{++}$  in these fluorides.

## INTRODUCTION

THE fluorides  $\text{CaF}_2$ ,  $\text{SrF}_2$ , and  $\text{BaF}_2$  belong to the space group  $O_h^5$  and are expected to have one infrared active transverse optical mode (TO) of vibration. At the present time the fundamental reststrahl frequency, TO at zero wave vector, has not been established with reasonable certainty. Although a number of measurements have been made in the infrared,<sup>1-6</sup> particularly on  $\text{CaF}_2$ , the data for the fundamental frequency are not consistent. The most recent measurements are those of Parodi<sup>5</sup> and of Heilmann.<sup>6</sup> Parodi measured the far infrared transmission of  $\text{CaF}_2$ ,  $\text{SrF}_2$ , and  $\text{BaF}_2$  powders and observed two absorption bands in each material. The bands in  $\text{CaF}_2$  are at 31 and 51.5  $\mu$ , in  $\text{SrF}_2$  at 40.6 and 69  $\mu$ , and in  $\text{BaF}_2$  at 43 and 73  $\mu$ . The longer wavelength absorption band in each case was interpreted as the TO resonance and that at the shorter wavelength as a harmonic or combination band. Heilmann presents reflection data between 17 and 38  $\mu$  for  $\text{CaF}_2$  measured with unpolarized radiation at normal incidence and with polarized radiation at an angle of incidence of 70°. From an analysis of these data and some transmission measurements on an evaporated film, he concluded that  $\text{CaF}_2$  has a relatively weak resonance near 30  $\mu$  in agreement with Parodi and that the wavelength of the TO resonance is between 38 and 40  $\mu$  with a probable value of 38.4  $\mu$ . In a recent paper<sup>7</sup> some measurements of Yoshinaga, Mitsuishi, and Yamada were quoted as placing the  $\text{CaF}_2$  fundamental resonance at  $\approx 37$   $\mu$ .

The fluorides  $\text{CaF}_2$ ,  $\text{SrF}_2$ , and  $\text{BaF}_2$  are receiving considerable attention since they are nearly ideal host lattices for paramagnetic ions. The ionic radii<sup>8</sup> of

$\text{Ca}^{++}$  (1.0 Å) and  $\text{Sr}^{++}$  (1.13 Å) are close to those of the ions of the rare-earth group and certain elements of the actinide group (e.g.,  $\text{U}^{3+}$ ). Alkaline earth fluorides doped with up to 1% of foreign ions can easily be prepared for optical and paramagnetic investigations.<sup>9</sup> The fluorescence of some of these ions shows clear evidence

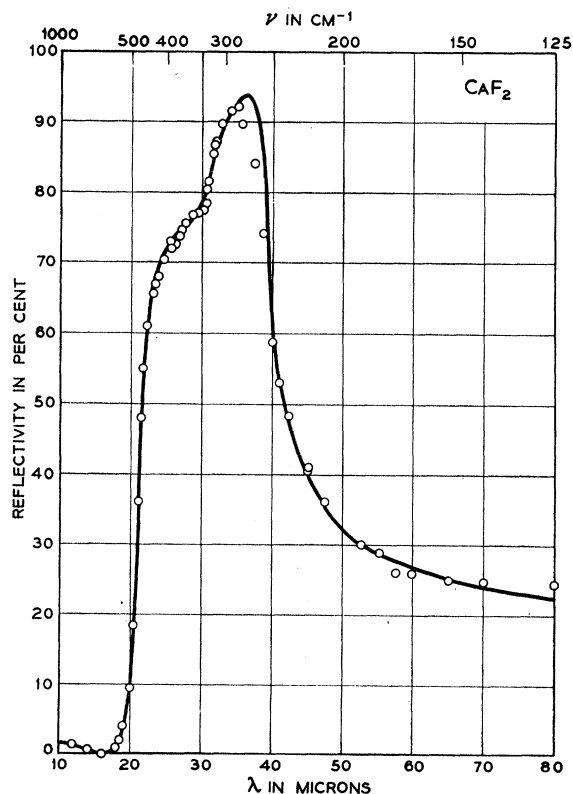


FIG. 1. Room temperature reflectivity of  $\text{CaF}_2$ . The data are indicated by the points. The curve is calculated from dispersion theory by using the parameters given in Table I.

<sup>1</sup> H. Rubens and G. Hertz, *Akad. Wiss. Ber. Sitzber.* **14**, 268 (1912).

<sup>2</sup> L. Kellner, *Z. Physik* **56**, 215 (1929).

<sup>3</sup> O. Reinkober and M. Bluth, *Ann. Physik* **6**, 785 (1930).

<sup>4</sup> F. Matossi and H. Brix, *Z. Physik* **29**, 303 (1934).

<sup>5</sup> M. Parodi, *Compt. rend.* **206**, 1717 (1938).

<sup>6</sup> G. Heilmann, *Z. Naturforsch.* **16a**, 714 (1961).

<sup>7</sup> T. Shimanouchi, M. Tsuboi, and T. Miyazawa, *J. Chem. Phys.* **35**, 1597 (1961); also see A. Mitsuishi, Y. Yamada, and H. Yoshinaga, *J. Opt. Soc. Am.* **52**, 14 (1962).

<sup>8</sup> L. Pauling, *The Nature of the Chemical Bond* (Cornell University Press, Ithaca, New York, 1960), 3rd ed., p. 514.

<sup>9</sup> P. Pringsheim, *Fluorescence and Phosphorescence* (Interscience Publishers, Inc., New York, 1949); B. Bleaney, P. M. Llewellyn, and D. A. Jones, *Proc. Phys. Soc. (London)* **B69**, 858 (1956); and W. Low, *Advances in Quantum Electronics*, edited by J. P. Singer (Columbia University Press, New York, 1961), p. 138.

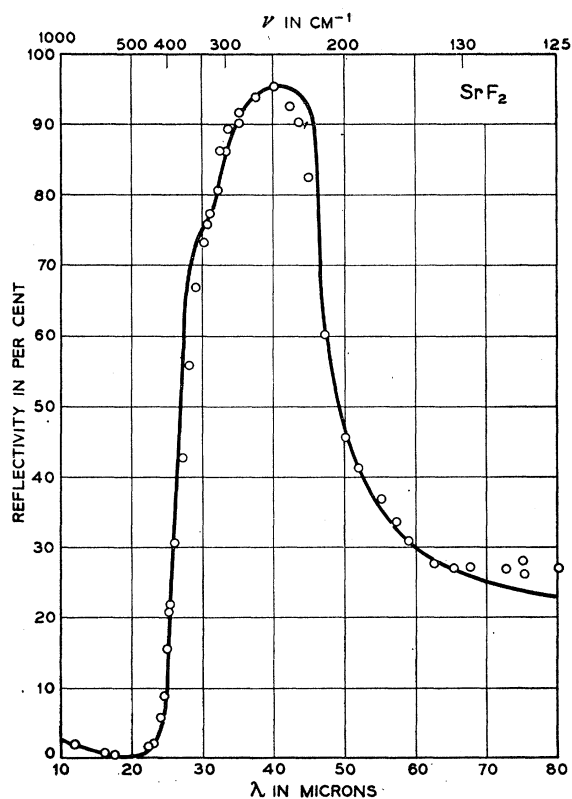


FIG. 2. Room temperature reflectivity of  $\text{SrF}_2$ . The data are indicated by the points. The curve is calculated from dispersion theory by using the parameters given in Table I.

of interactions between electronic transitions and lattice vibrations of the host crystal.<sup>10</sup> In the emission spectrum of  $\text{Sm}^{++}$ , for example, sharp emission lines ( $4f \rightarrow 4f$  transitions) are followed by a distinct group of satellite lines which are the result of the interaction with lattice vibrations. It is, therefore, of importance to obtain information concerning the vibrational spectrum of the pure alkaline earth fluorides.

The transmission as a function of frequency and temperature has been measured on  $\text{CaF}_2$ ,  $\text{SrF}_2$ , and  $\text{BaF}_2$  single crystals on the high-frequency side of the reflectivity band. The reflectivity has been measured from  $10 \mu$  through the dispersion range to  $80 \mu$ . Applying classical dispersion analysis to the reflectivity data, the frequency and resonance strength of the  $TO$  mode are obtained and from a combination band the frequency of a phonon, assumed to be acoustical, could be estimated. The frequency of the  $TO$  phonon agrees very well with the observed separation of one of the satellite lines for  $\text{Sm}^{++}$  in each of the fluorides. From the transmission measurements and the dispersion analysis of the reflectivity, the optical constants are obtained between  $10$  and  $80 \mu$  ( $1000$  and  $125 \text{ cm}^{-1}$  where frequency is given in units of  $\text{cm}^{-1}$ ).

<sup>10</sup> D. L. Wood and W. Kaiser, Phys. Rev. **126**, 2079 (1962).

## EXPERIMENTAL

Room temperature reflectivity measurements at near normal incidence have been made for each of the three fluorides. The equipment and experimental technique used in these measurements have been previously described in considerable detail.<sup>11</sup> Since the fluorides have cubic symmetry, the spectrometer beam was not polarized. One large area surface of each sample was polished by using standard metallographic polishing methods. The back surface was roughened so as to eliminate the contribution of multiple internal reflections to the reflectivity. The measured reflectivity of  $\text{CaF}_2$ ,  $\text{SrF}_2$ , and  $\text{BaF}_2$  is shown by the points in Figs. 1, 2, and 3, respectively.

At frequencies above the reflection band, the crystals are sufficiently transparent to allow direct transmission measurements. These measurements were made on a set of single crystals between  $\approx 5$  and  $0.1 \text{ mm}$  in thickness. Data were taken at  $300$ ,  $77$ ,  $65$ , and in some cases  $5^\circ\text{K}$ . Similar to a number of other ionic crystals,<sup>12</sup> it was observed that below  $77^\circ\text{K}$  the transmission changed only very slightly with temperature. The absorption

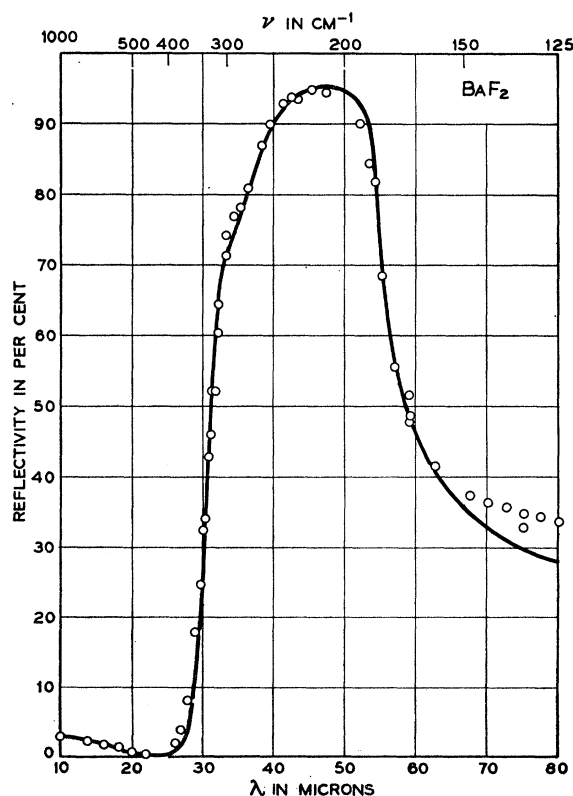


FIG. 3. Room temperature reflectivity of  $\text{BaF}_2$ . The data are indicated by the points. The curve is calculated from dispersion theory by using the parameters given in Table I.

<sup>11</sup> W. Spitzer, R. Miller, D. Kleinman, and L. Howarth, Phys. Rev. **126**, 1710 (1962).

<sup>12</sup> G. O. Jones, D. H. Martin, P. A. Mawer, and C. H. Perry, Proc. Roy. Soc. (London) **261**, 10 (1961).

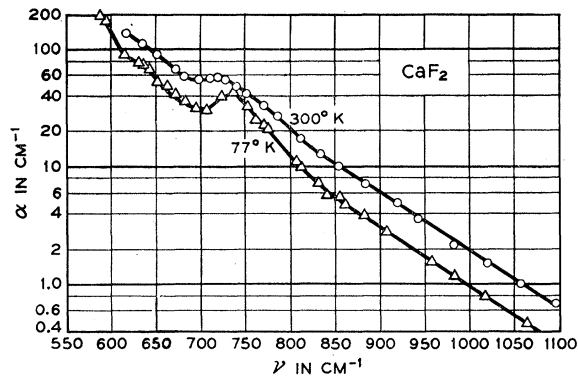


FIG. 4. Absorption coefficient of  $\text{CaF}_2$  at 300 and 77°K.

coefficient  $\alpha$  ( $\text{cm}^{-1}$ ) was calculated from the transmission according to the equation

$$T = (1-R)^2 e^{-\alpha x} / (1-R^2 e^{-2\alpha x}),$$

where  $R$  is the reflectivity and  $x$  the sample thickness in cm. The room temperature and 77°K values of  $\alpha$  for the fluorides are shown by the points in Figs. 4-6.

According to the literature, the value of the static dielectric constant  $\epsilon_0$  of  $\text{SrF}_2$ <sup>13</sup> is larger than that for either  $\text{CaF}_2$  or  $\text{BaF}_2$ .<sup>14</sup> From the results of the dispersion analysis of the reflectivity it was apparent that the large  $\epsilon_0$  for  $\text{SrF}_2$  was not compatible with the present data. Therefore, the  $\epsilon_0$  for the three crystals was re-measured (at  $10^3$  and  $10^6$  cps) by using a conventional capacity bridge. The values of  $\epsilon_0$  measured on thin ( $\approx 1$  mm) single crystal plates are listed as  $\epsilon_0(\text{exp})$  in Table I. The measurements are estimated to have an accuracy of 5%. The value  $\epsilon_0(\text{exp})=6.6$  for  $\text{SrF}_2$  deviates substantially from the published value of 7.69. The  $\epsilon_0(\text{exp})$  values given here for  $\text{CaF}_2$  and  $\text{BaF}_2$  are in good agreement with previously published values given in Table I as  $\epsilon_0$  (literature).

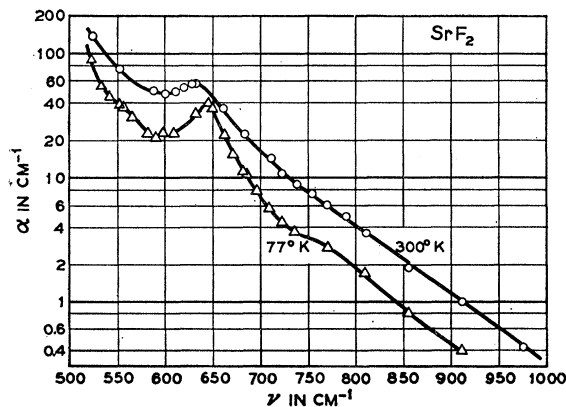


FIG. 5. Absorption coefficient of  $\text{SrF}_2$  at 300 and 77°K.

<sup>13</sup> K. Hojendahl, Kgl. Danske Videnskab. Selskab, Mat.-fys. Medd. **16**, 2 (1938).

<sup>14</sup> American Institute of Physics Handbook (McGraw-Hill Book Company, Inc., New York, 1957), Vol. 5, p. 115.

## DISCUSSION

In recent years it has been demonstrated for several materials that reflectivity data such as those of Figs. 1-3 can be accurately represented by classical dispersion theory.<sup>15-18</sup> Since the theory and technique of curve fitting have been discussed extensively in recent literature, no discussion of the method will be presented here. According to the theory, the real and imaginary parts of the complex dielectric constant,  $\epsilon'$  and  $\epsilon''$ , are given by

$$\epsilon' = n^2 - k^2 = \epsilon_\infty + \sum_j \frac{4\pi\rho_j\nu_j^2}{(\nu_j^2 - \nu^2) + \gamma_j^2\nu^2\nu_j^2}$$

and

$$\epsilon'' = 2nk = \sum_j \frac{\gamma_j\nu\nu_j}{(\nu_j^2 - \nu^2)^2 + \gamma_j^2\nu^2\nu_j^2},$$

where  $n$  is the refractive index,  $k$  the extinction coefficient,  $\epsilon_\infty$  the high-frequency limiting value of the di-

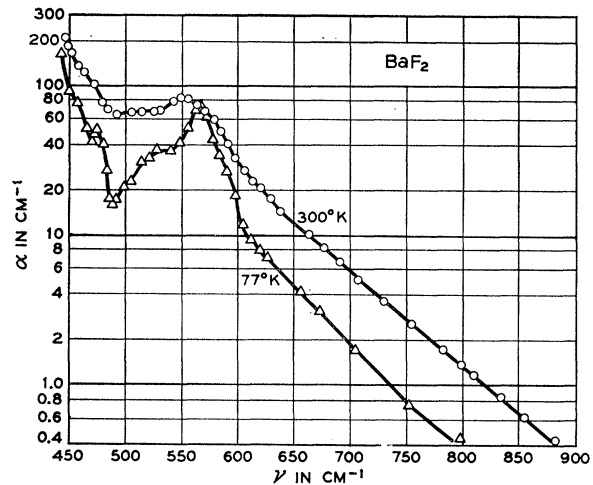


FIG. 6. Absorption coefficient of  $\text{BaF}_2$  at 300 and 77°K.

electric constant,  $4\pi\rho_j$  the strength of the  $j$ th resonance,  $\gamma_j$  the width or damping constant for the  $j$ th resonance, and  $\nu_j$  the resonance frequency. It was found that the reflectivity data could be quantitatively fitted throughout most of the measured spectral range with one strong and one weak resonance for each case. The curves of best fit obtained to date are given in Figs. 1-3, and the parameters used to obtain these curves are listed in Table I. The values of  $\alpha$  listed in the table are the peak values of the absorption band. In all three cases a relatively poor fit is seen in a narrow spectral region on the long-wavelength side of the reflectivity peak. This discrepancy is not surprising since the sample surfaces

<sup>15</sup> W. Spitzer, D. Kleinman, and D. Walsh, Phys. Rev. **113**, 127 (1959).

<sup>16</sup> W. Spitzer, D. Kleinman, and C. Frosch, Phys. Rev. **113**, 133 (1959).

<sup>17</sup> D. Kleinman and W. Spitzer, Phys. Rev. **118**, 110 (1960).

<sup>18</sup> W. Spitzer and D. Kleinman, Phys. Rev. **121**, 1324 (1961).

were mechanically polished. The same effect was observed on polished SiC surfaces<sup>15</sup> and shown to be the result of a thin ( $\sim 1 \mu$ ) damaged surface layer. It is also noted that particularly in the cases of  $\text{SrF}_2$  and  $\text{BaF}_2$ , the calculated curve falls below the measured points at the longest wavelengths. This difference, which exceeds the experimental error in the measurements ( $\pm 2\%$  reflectivity at  $\lambda = 80 \mu$ ) is also indicated by comparing the  $\epsilon_\infty + \sum 4\pi\rho$  values with those of  $\epsilon_0(\text{exp})$  from capacity measurements as given in Table I. While the two values are in good agreement for  $\text{CaF}_2$ , the difference in the values for  $\text{SrF}_2$  and for  $\text{BaF}_2$  indicate the presence of some additional absorption at still lower frequency for these two materials. At present, the source of this additional absorption is not understood. The optical con-

TABLE I. A list of the parameters used to calculate the dispersion curves of Figs. 1, 2, and 3.  $\alpha_1$  and  $\alpha_2$  are the peak values of the absorption coefficient due to the  $\nu_1$  and  $\nu_2$  resonances, respectively. Also listed are the frequencies of the longitudinal optical phonon, an acoustical phonon, and an absorption band observed in Figs. 4, 5, and 6. The values of the low-frequency dielectric constant as obtained from capacity measurements are given as  $\epsilon_0(\text{exp})$ .

	$\text{CaF}_2$	$\text{SrF}_2$	$\text{BaF}_2$
$\nu_1(TO)$ , $\text{cm}^{-1}$	257	217	184
$\lambda_1$ , $\mu$	38.9	46.1	54.3
$\gamma_1$	0.018	0.017	0.020
$4\pi\rho_1$	4.20	4.00	4.50
$\alpha_1$ (peak value), $\text{cm}^{-1}$	$3.9 \times 10^4$	$3.3 \times 10^4$	$2.8 \times 10^4$
$\nu_2$ , $\text{cm}^{-1}$	328	316	278
$\lambda_2$ , $\mu$	30.5	31.7	36.0
$\gamma_2$	0.35	0.25	0.30
$4\pi\rho_2$	0.40	0.07	0.07
$\alpha_2$ (peak value), $\text{cm}^{-1}$	$1.7 \times 10^3$	$0.5 \times 10^3$	$0.4 \times 10^3$
$\epsilon_\infty$	2.045	2.07	2.16
$\epsilon_0 = \epsilon_\infty + \sum 4\pi\rho$	6.65	6.14	6.73
$\epsilon_0(\text{exp})$	6.7	6.6	7.2
$\epsilon_0$ (literature) <sup>a</sup>	6.8	7.69	7.33
$\nu_{LO}$ , $\text{cm}^{-1}$	463	374	326
$\nu_{ao}$ , $\text{cm}^{-1}$	71	99	94
$\nu_3$ , $\text{cm}^{-1}$	720	630	550
$\nu_1 + \nu_{LO}$ , $\text{cm}^{-1}$	720	591	510
$3\nu_1$ , $\text{cm}^{-1}$	770	650	552

<sup>a</sup> See references 12 and 13.

stants  $n$  and  $k$  deduced from the analysis of the reflectivity data are given in Figs. 7 and 8.

The strong resonances ( $\nu_1$  of Table I) at 257, 217, and 184  $\text{cm}^{-1}$  for  $\text{CaF}_2$ ,  $\text{SrF}_2$ , and  $\text{BaF}_2$ , respectively, are identified as the optically active  $TO$  resonances. The  $TO$  frequency for  $\text{CaF}_2$  is in reasonable agreement with the value given by Heilmann<sup>6</sup> and by Yoshinaga *et al.* The  $TO$  values for the three fluorides are not in agreement with those given by Parodi.<sup>5</sup> The frequency of the longitudinal optical phonon of zero wave vector can be estimated from the Lyddane, Sachs, Teller relation,<sup>19</sup>

$$\nu_{LO} = \nu_{TO} (\epsilon_0 / \epsilon_\infty)^{1/2},$$

<sup>19</sup> R. Lyddane, R. Sachs, and E. Teller, Phys. Rev. **59**, 673 (1941). For a discussion concerning the applicability of this expression for  $\text{CaF}_2$ , see S. Ganisan and R. Srinivasan, Can. J. Phys. **40**, 74 (1962).

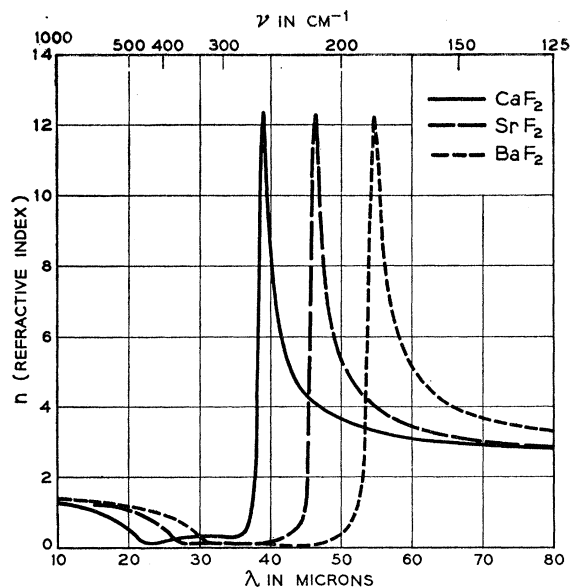


FIG. 7. Refractive index for each of the fluorides as obtained from the dispersion analysis of the reflectivity.

and the  $\nu_{LO}$  for each material is also given in Table I. The second resonance used in each of the calculations (see  $\nu_2$  of Table I) is between one and two orders of magnitude weaker than the main resonance. If the  $\nu_2$  resonance is a two-phonon combination band involving the  $TO$  mode, then the frequency of the second phonon, probably acoustical, is given in Table I as  $\nu_{ao}$ . The  $\nu_2$  frequency of  $\text{CaF}_2$  is close to that given by Heilmann<sup>6</sup> and by Parodi.<sup>5</sup> However, the  $\nu_2$  frequencies for  $\text{SrF}_2$  and  $\text{BaF}_2$  do not agree with those given by Parodi. In the room temperature absorption curves for these

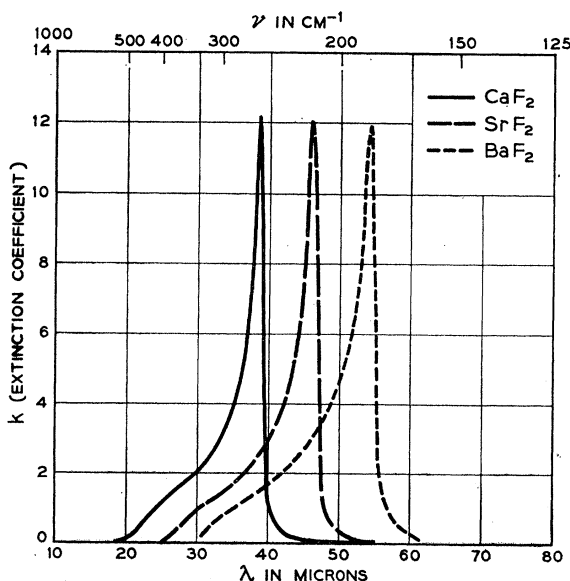


FIG. 8. Extinction coefficient for each of the fluorides as obtained from the dispersion analysis of the reflectivity.

crystals (Figs. 4–6) one weak absorption band is observed in each case. The frequency of this band, which is called  $\nu_3$  in Table I, is close to both  $\nu_1(TO) + \nu_{LO}$  and  $3\nu_1$ . After subtracting out the background absorption, the strength of this band is approximately an order of magnitude less than the two phonon combination band at  $\nu_2$ . Exact agreement is not expected between the values of  $3\nu_1$  (or  $\nu_1 + \nu_{LO}$ ) and  $\nu_3$  since  $\nu_1$  is the  $TO$  frequency at zero wave vector which may differ considerably from the  $TO$  frequency in other parts of Brillouin zone. The question may be raised as to why the  $2\nu_1$  was not observed for any of these materials. The frequency of this band places it beyond the spectral range of the transmission measurements, and it occurs very close to the minimum in the reflectivity curves. Assuming the strength of this band to be the same as that of the  $\nu_2$  band, calculations showed that it would be very difficult to observe in the reflectivity.

As previously indicated, several sharp emission lines of  $\text{Sm}^{++}$  in  $\text{CaF}_2$ ,  $\text{SrF}_2$ , and  $\text{BaF}_2$  were followed by a group of lines which were considered to be the result of

interactions with the host lattice. One of the two strongest satellite lines in  $\text{SrF}_2$  and  $\text{BaF}_2$  is separated from the sharp electronic (magnetic dipole) transition by 216 and 186  $\text{cm}^{-1}$ , respectively. These values agree very well with the measured  $TO$  frequencies of 217  $\text{cm}^{-1}$  and 184  $\text{cm}^{-1}$ , indicating that the fluorescence occurs to a vibrational level above the terminal electronic state. In  $\text{SrF}_2$ , a weak satellite line with a separation of  $\approx 90 \text{ cm}^{-1}$  is observed and a relation to the  $\nu_{ac} = 99 \text{ cm}^{-1}$  discussed above is likely. The fluorescence of  $\text{Sm}^{++}$  in  $\text{CaF}_2$  is quite different from that in  $\text{SrF}_2$  and  $\text{BaF}_2$ . The major emission line of  $\text{Sm}^{++}$  in  $\text{CaF}_2$  (14 118  $\text{cm}^{-1}$ ) corresponds to an electric dipole transition involving a lattice vibration. The vibrational structure following this intense line has several distinct maxima. One of these maxima is separated from the main fluorescent line by 250  $\text{cm}^{-1}$  (at 77°K), which is close to the observed  $TO$  frequency of 257  $\text{cm}^{-1}$ . Therefore, vibrational levels occur for  $\text{Sm}^{++}$  in all three fluorides which can be identified with the  $TO$  mode of vibration of the host lattice.

## Weak-Field Magnetoresistance of Impurity Conduction in *n*-Type Germanium\*

NOBUO MIKOSHIBA†

*Institute for the Study of Metals, University of Chicago, Chicago, Illinois*

AND

SHUN-ICHI GONDA

*Electrotechnical Laboratory, Nagatacho, Tokyo, Japan*

(Received March 6, 1962; revised manuscript received May 23, 1962)

The coefficients  $B$ ,  $C$ , and  $D$  of the weak-field magnetoresistance in *n*-type germanium are calculated in the phonon-induced hopping region at low temperatures. The shrinking of each donor wave function by a magnetic field decreases the transition probability of electrons from a donor site to an unoccupied one and gives rise to a magnetoresistive effect. The phase difference produced by the field between two neighboring donor wave functions contributes to the magnetoresistance to the same order of magnitude as the effect of the shrinking. The results show some characteristic properties of  $B$ ,  $C$ , and  $D$  different from those of electrons in the conduction band: (1) The absolute magnitude of the coefficients is larger for specimens with smaller carrier mobility; (2) the magnitude is much larger than that expected from the usual transport theory of conduction electrons; (3) the isotropic part of the coefficients  $B$  is the largest; and (4) the coefficient  $D$ , which represents the anisotropy of the electronic motion, is the smallest among the three coefficients. These properties are in qualitative agreement with recent experiments in a slightly higher impurity concentration range in *n*-type germanium.

### I. INTRODUCTION

THE theory of weak-field magnetoresistance was developed for conduction electrons in *n*-type germanium by Abeles and Meiboom<sup>1</sup> and Shibuya.<sup>2</sup> By introducing a many-valley model with an anisotropic effective mass in each valley, verified by cyclotron resonance experiments,<sup>3</sup> they could explain

the large anisotropy of the magnetoresistance in *n*-type germanium.

A phenomenological relation<sup>4</sup> between the electric field  $\mathbf{E}$  and the electric current  $\mathbf{J}$  in a weak magnetic field  $\mathbf{H}$ ,

$$\mathbf{E} = \rho_0 [\mathbf{J} + A\mathbf{J} \times \mathbf{H} + B\mathbf{H}^2\mathbf{J} + C\mathbf{H}(\mathbf{J} \cdot \mathbf{H}) + D\mathbf{M}\mathbf{J}], \quad (1.1)$$

holds generally in cubic crystals such as germanium, where  $\rho_0$  is the resistivity in zero magnetic field and

\* Supported in part by the National Science Foundation.

† On leave of absence from the Electrotechnical Laboratory, Nagatacho, Tokyo, Japan, where this work was begun.

<sup>1</sup> B. Abeles and S. Meiboom, *Phys. Rev.* **95**, 31 (1954).

<sup>2</sup> M. Shibuya, *Phys. Rev.* **95**, 1385 (1954).

<sup>3</sup> G. Dresselhaus, A. F. Kip, and C. Kittel, *Phys. Rev.* **98**, 368 (1955).

<sup>4</sup> F. Seitz, *Phys. Rev.* **79**, 372 (1950).